Scientific Research Publishing

Advances in Nanoparticles, 2023, 12, 147-159
https://www.scirp.org/journal/anp
ISSN Online: 2169-0529
ISSN Print: 2169-0510

Magnetite Nanoparticles Coated with Synthetic Polymer for Hyperthermia Application: Review

Abdelaziz Sabik

Department of Physics, College of Sciences, Imam Mohammad Ibn Saud Islamic University (IMISU), Riyadh, Saudi Arabia
Email: amsabik@imamu.edu.sa

How to cite this paper: Sabik, A. (2023) Magnetite Nanoparticles Coated with Synthetic Polymer for Hyperthermia Application: Review. *Advances in Nanoparticles*, **12**, 147-159.
https://doi.org/10.4236/anp.2023.124012

Received: November 1, 2023
Accepted: November 26, 2023
Published: November 29, 2023

Abstract

Hyperthermia treatment using appropriate magnetic materials in an alternating magnetic field to generate heat has been proposed as a low-invasive cancer treatment method. Magnetite iron oxide nanoparticles (Fe_3O_4) are expected to be an appropriate type of magnetic material for this purpose due to its biocompatibility. Several polymers are used to Fe_3O_4 MNPs to avoid or decrease agglomeration, and in most cases increase dispersion stability. In this review, we will give briefly how these coated magnetite nanoparticles (PMNPs) are synthesized in the first part. The main characterization techniques usually used to study the properties of these MNPs are prseneted in the second part. Finally, most recent results on the heating ability of polymeric coated magnetite nanoparticles (PMNPs) are given in the last part of this review.

Keywords

Magnetic Hyperthermia, Polymers, Iron Oxides, Nanoparticles

1. Introduction

Magnetic hyperthermia therapy is a cancer treatment method which uses the ability of magnetic nanoparticles to generate heat when exposed to an alternating magnetic field. The elevation in the temperature of the tissue induces few physical and physiological changes. As well known, the cancer tissue is more thermosensitive than normal tissue at between 42˚C and 45˚C. Injection of coated magnetic nanoparticles near the tumor followed by application of an alternating magnetic field for 15 to 60 min to gain and maintain a temperature in the range of 42˚C - 46˚C is enough to kill completely cancer cells with minimal injury to normal cells.

The mechanisms for heating magnetic nanoparticles with an AC magnetic

field include three types of loss processes (hysteresis losses, Néel relaxation, and Brownian relaxation). The relative contribution of each process depends strongly on the crystal size and composition of the particles. Nanoparticles with core diameters of less than 20 nm or so, as used in most magnetic fluid hyperthermia applications, are single-domain particles, meaning that they consist of only a single organized crystal. In such small nanoparticles, magnetization relaxation is governed by a combination of the external rotation (Brownian) and internal (Néel) diffusion of the particle's magnetic moment, with negligible contribution of hysteresis loss.

Magnetic nanoparticles (MNPs), within the size of 1 nm and 100 nm, have been an important nanomaterial for science and technology in the past three decades. Their unique characteristics such as high surface to volume ratio and size-dependent magnetic properties are drastically different from those of their bulk materials. One of the most important MNPs is magnetite (Fe_3O_4), which is more widely used than other magnetic nanoparticles due to its biocompatibility [1] and low cost. Its structure gives it special properties so that it can be used in many medical, pharmaceutical and therapeutic applications [2] [3] [4] [5]. To prevent the agglomeration of magnetic nanoparticles and increase dispersion stability, it is necessary to modify their surfaces with biocompatible coatings [6]. The coating of nanoparticles with biocompatible materials has been studied by many research groups [7] [8] [9] [10].

In this review, we will give briefly how these coated magnetite nanoparticles are synthesized, the different characterization techniques used to study the physico-chemical properties and finally few examples of heating ability of polymeric coated magnetic nanoparticles (PMNPs).

2. Preparation of Magnetic Nanoparticles Coating with Polymer by Co-Precipitation Method

There are many other methods (chemical or physical), which allow the synthesis of polymerated coated magnetic nanoparticles such as hydrothermal, sol-gel, co-precipitation, ball milling, etc. We will review briefly in this paper magnetic nanoparticles coated by polymers synthesized by these methods.

For example, the simplest and the most used one is the co-precipitation method in which no organic solvents are required [11]. The typical co-precipitation method for the preparation of magnetite is as follow: the salt of "$FeCl_2{\cdot}4H_2O$" was added to a distilled water that was previously purged by nitrogen, and $FeCl_3{\cdot}6H_2O$ was added after the good dissolution of salt. In this synthesis, the stoichiometry of "$FeCl_2{\cdot}4H_2O$"/"$FeCl_3{\cdot}6H_2O$" was 1/2. Separately, a polymer solution was prepared and sonicated with ultrasonic bath. The solution containing polymer was mixed with the metallic ion solution while bubbling N_2 gas, and NH_3 aqueous solution was added dropwise till a pH > 8 was achieved and stirred for 1 hour. The sample was dried in an oven and then ground by a mortar.

It was well known that $Fe(OH)_2$ and $Fe(OH)_3$ are formed at pH > 8 by the hydroxylation of the ferrous and ferric ions under anaerobic conditions [12]. The

possible reactions for the formation of Fe_3O_4 MNPs are as follows:

$$Fe^{3+} + 3OH^- \rightarrow Fe(OH)_3$$

$$Fe(OH)_3 \rightarrow FeOOH + H_2O$$

$$Fe^{2+} + 2OH^- \rightarrow Fe(OH)_2$$

$$2FeOOH + Fe(OH)_2 \rightarrow Fe_3O_4 \downarrow + 2H_2O$$

It is essential to note that the whole reaction mixture be free of oxygen, otherwise magnetite can be oxidized to ferric hydroxide (γ-Fe_2O_3) in the reaction medium.

3. Characterization Methods

There is a wide range of experimental techniques to study magnetic properties of PMNPs. We focus in this part on the main techniques.

3.1. Dynamic Light Scattering (DLS)

It uses Brownian motion to provide information about the hydrodynamic radius (R_h), size distribution (polydispersity, PDI), and the colloidal stability of nanoparticles in solution [13]. Quite often, PDI values from 0.1 to 0.25 are used to confirm a narrow size distribution, whereas a PDI value higher than 0.5 is often referred to as a broad distribution [14]. The size distributions resulting from DLS are of high value concerning the aggregation behavior prior to and after surface modification as well as the apparent changes in nanoparticle size. However, this method merely provides an average value.

3.2. Transmission Electron Microscopy (TEM)

It provides supplementary information about size, shape, and shell thickness of individual nanoparticles. Especially regarding the latter case, TEM investigations can be easily used to get an impression about the effect of the polymeric shell on the MNP aggregation behavior. However, the results have to be interpreted with care as aggregation of the nanoparticles and damaging of organic nanostructures can occur during drying processes. For this reason, TEM and DLS are often used in combination [15].

3.3. The Zeta Potential

It has tremendous influence on suspension stability of nanoparticles, eventual secondary aggregation, or any interaction with other materials. The zeta potential is measured by laser doppler velocimetry as the electrophoretic mobility of the respective colloidal suspension and represents the potential at the slipping plane of a particle in solution during movement [16]. In general, high values result in an improved stabilization, while a value close to zero typically leads to fast aggregation and eventual precipitation in aqueous media.

3.4. X-Ray Diffraction (XRD)

Powder x-ray investigations are most often used to obtain information about the

crystal structure and phase of the magnetic core. This method provides information regarding the crystallinity of MNPs, as well as their average crystallite size.

The average crystallite size, D, is calculated from Scherer's equation [17] without considering the effect of lattice strains as

$$D = \frac{K\lambda}{\beta \cos\theta} \tag{1}$$

where λ is the incident wavelength (1.5406 Å), θ is the Bragg angle (in degree), K is a constant whose value is approximately 0.9 and β (rad) is the full width at half maximum (FWHM) of a diffraction peak or integral breadth [18] [19].

3.5. Vibrating Sample Magnetometry (VSM)

It determines the magnetic properties of magnetic nanoparticles. The magnetic properties can be used to estimate the amount of diamagnetic material in the sample, for example the organic material representing the shell. Comparison of the weight of a sample with the corresponding magnetic properties allows calculation of the amount of diamagnetic organic material. Furthermore, this method validates whether the investigated nanoparticles are (still) superparamagnetic. The magnetic parameters (*i.e.*, saturation magnetization (M_s), remanence magnetization (M_r), and coercivity (H_c)) are determined from the M-H curves.

3.6. Thermogravimetric Analysis (TGA)

It can be used to determine the overall amount of organic material located at the surface of inorganic nanoparticles. Thereby, one clear benefit is that small samples amounts can be used to verify the presence of organic surface coatings. This tool is of utmost interest when it comes to a quantitative evaluation of coating processes and/or the determination of biological adsorption processes [20].

4. Heating Efficiency

The heat generated per unit gram of magnetic material and per unit time under alternating magnetic field is known as specific absorption rate (SAR). Previous reports showed that the SAR values of the nanoparticles could be affected by several parameters such as sample preparation method, size of nanoparticles, magnetic properties, the amplitudes and frequency of the applied field, coating, etc.

The amount of heat generated by magnetic nanoparticles is normally quantified in terms of the SAR, which can be calculated by:

$$\mathrm{SAR} = \frac{\rho C_w}{m_{NP}}\left(\frac{\Delta T}{\Delta t}\right) \tag{2}$$

where C_w is the specific heat capacity of water (4.185 J/g k), ρ is the density of the colloid, m_{NP} is the concentration of the magnetic nanoparticles in the suspension and $\Delta T/\Delta t$ is the initial slope of the time-dependent temperature curve. This gives SAR the units W/g [21]. The fundamental problem with this parameter is

that SAR is extrinsic and varies depending on both H (field strength) and f (frequency). Therefore, measurements are only comparable if made on the same machine that has the same H and f [22].

5. Recent Results on Heating Ability of Coated Magnetite Nanoparticles

Many research groups investigated the heating ability of polymeric coated magnetic nanoparticles (PMNPs) as function of many parameters such as preparation methods, field amplitude and frequency. We will summarize the most recent works, which investigate the heating efficiencies of these PMNPs.

El Boubou *et al.* [23] reported the preparation of different Polymerylated MNPs (PMNPs) capped with five widely used polymers (PVP, PEG, Dextran, HA, and PAA) synthesized by hydrothermal method. The main results are summarized in Table 1. Figure 1(a) depicted the magnetization-field (M-H) curves recorded at room temperature for the different PMNPs. All the samples show superparamagnetic behavior with negligible coercivity and remanence. The saturation magnetization (Ms) obtained for PVP-MNPs, PEG-MNPs, HA-MNPs, Dextran-MNPs, and PAA-MNPs were found to be equal to 72, 62, 61, 49 and 9.5 emu/g, respectively. The high saturation makes this PMNPs promising for heat dissipation under alternating magnetic. The authors investigated the heating ability under alternating magnetic field of amplitude 170 Oe and frequency of 332 kHz (Figure 1(b)). They found that all the PMNPS show high heating abilities and reach magnetic hyperthermia temperatures (42˚C) in relatively short times. SAR values were found to be equal to 160, 70, 40, 36 and 2 W/g for PVP, PEG, HA, Dextran, and PAA-coated MNPs respectively. PVP-MNPs showed the highest SAR (160 W/g) compared to other samples (Figure 1(c)). El Boubbou and his collaborators investigated the ability of these PMNPs to kill cancer cells under AMF. They found that PVP-MPNs were efficient to treat breast cancer cell with more than 90% cell killed after applying magnetic field for thirty minutes (Figure 1(d)).

Algessair *et al.* [24] studied the self-heating ability of PAA-coated magnetite (Fe_3O_4) nanoparticles as function of concentration of PMNPs, field amplitude and frequency. The authors characterize the as-prepared PMNPs by many techniques including TEM, FTIR, DLS, TGA, and VSM. TEM images depicted in Figure 2(a) show that the MNPs are uniform colloidal with ultra-small size of

Table 1. Main parameters deduced from the measurements [23].

Sample	Av. crystallite size (nm)	core size (nm)	Morphology	Hydrodynamic size (nm)	PDI	Zeta potential (mV)	Polymer	Fe^{2+}	Ms (emu/g)	42 (deg.) (seconds)	45 (deg.) (seconds)	SAR (W/g)	ILP (nH·m²/kg)
Bare-MNPs		12.5	quasi-spherical	150	0.232	1.15	2 (wt%)	70.9 (wt%)					
PVP-MNPs		11	quasi-spherical	145	0.202	10	15 (wt%)	61.5 (wt%)	72	90	120	160	2.6
PEG-MNPs		9.5	quasi-spherical	120	0.27	−40	18 (wt%)	59.3 (wt%)	62	180	260	70	1.15
PAA-MNPs		5	quasi-spherical	75	0.241	−45	60 (wt%)	28.9 (wt%)	10	Not reached	Not reached	2	0.03

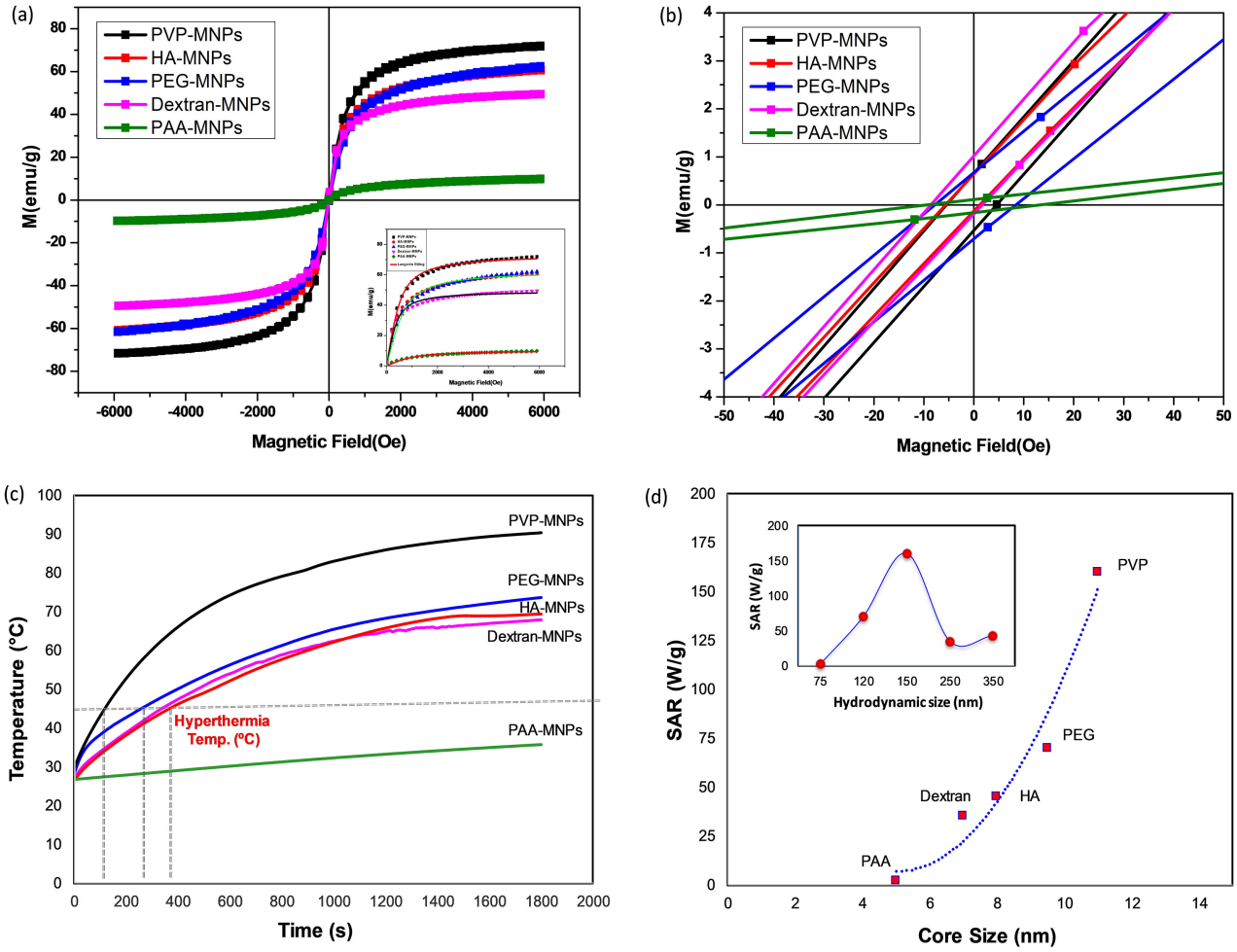

Figure 1. (a) Field-dependent magnetization (M-H) curves for the various PMNPs. (b) Magnetization curves at low field from 50 Oe to 50 Oe. (c) Hyperthermia heating efficiency depicted by a plot of temperature increase vs. time of the different PMNPs (10 mg mL^{-1}) under an alternating magnetic field (H0 = 170 Oe and frequency = 332.8 kHz). (d) Plot of SAR values as a function of TEM core size [23].

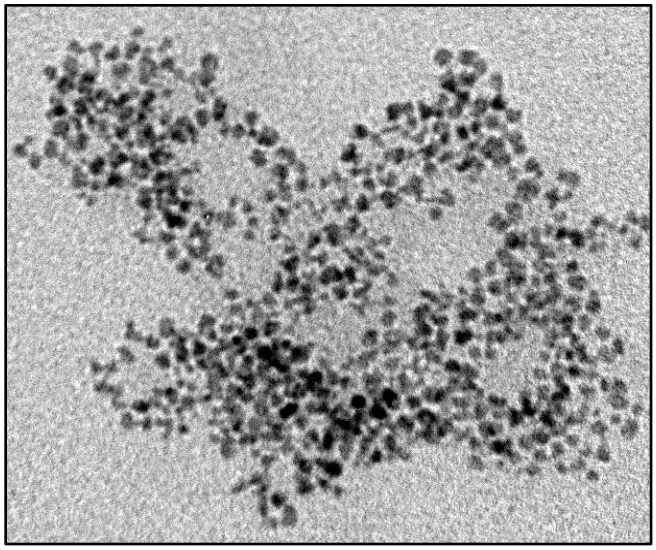

(a)

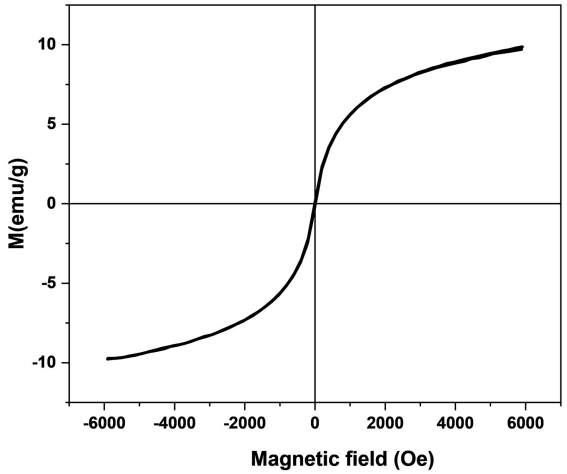

(b)

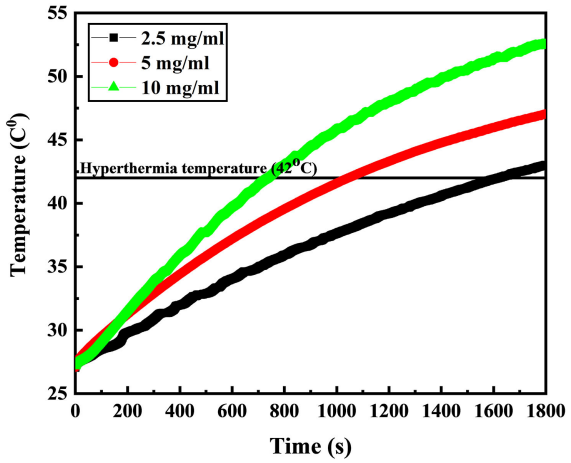

(c)

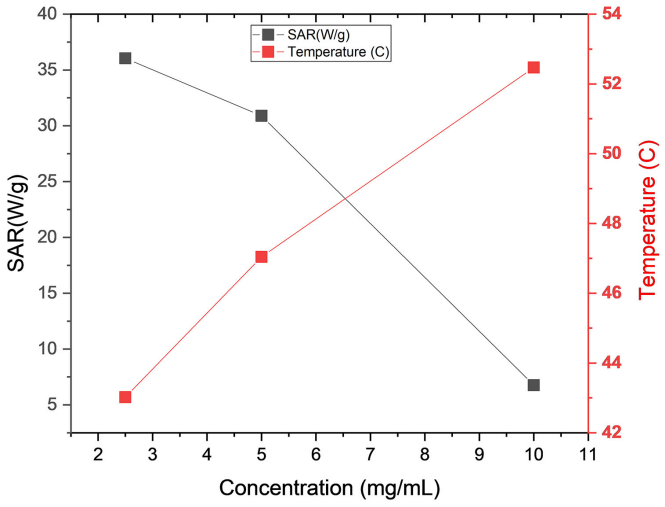

(d)

Figure 2. (a) TEM image, (b) Magnetization at room temperature, (c) Hyperthermia heating efficiency at different concentration under an alternating magnetic field (H0 = 170 Oe and frequency = 332.8 kHz), (d) Plot of SAR and maximum temperature [24].

MNPs 5 nm, while magnetization at room temperature reveals superparamagnetic behavior (Figure 2(a), Figure 2(b)). Heat dissipate by the MNPs under AMF was investigated as function of concentration of MNPs, field amplitude and frequency. They observed that temperature rise increases with increasing concentration (Figure 2(c)). It can be seen also that magnetic hyperthermia temperature is reached in short time for all the concentration. Interestingly, the authors observed that SAR decreases with increasing concentration of MNPs (Figure 2(d)). This decrease of SAR with increasing the concentration of PAA-MNPs is due to the enhancement of interparticle dipolar interactions. Many researchers reported similar results and explained such behavior by the interparticle dipolar interaction, which could influence the heating ability of MNPs by reducing Neel-Brownian relaxation times [25] [26].

Miyazaki *et al.* [27] investigated the effect of different types of polymers on the size of MNPs, their magnetization and the SAR for magnetic hyperthermia. The main structural, magnetic and heating ability parameters are summarized in Table 2 below. They observed that the size of MNPs decreased with increasing polymer molecular weight except for polyethyleneimine. All the coated samples show a superparamagnetic behavior as indicated in Figure 3(a). Heating efficiency under AMF reveals that the polymeric MNPs reached a high temperature, but the SAR values are very low (Figure 3(b)). Optimization of some parameters such as the size, the percentage of polymers will increase this value and make them good candidate for hyperthermia.

Table 2. Parameters deduced from structure, magnetic and heating characterization [27].

Sample	Av. crystallite size (nm)	core size (nm)	Morphology	type of polymer	Coordination complex	stability constant	Zeta potential (mV)	Fe^{2+} (conc/mM)	Ms (emu/g)	SAR (W/g)	
Bare-MNPs	21.3		spherical shape	//////////	//////////	//////////	39.6	0.072	55.8	3	desirable for hyperthermia
PEG 200	15.5	10 - 20	spherical shape	non ionic polymer	//////////	//////////	//////////	0.072	69.5	2.3	
PEG 600	13.8	10 - 20	spherical shape	non ionic polymer	//////////	//////////	//////////	0.072	//////////	2.7	desirable for hyperthermia
PEG 6000	11	10 - 20	spherical shape	non ionic polymer	//////////	//////////	−17.4	0.072	38.1	4.5	desirable for hyperthermia
PSSS 300,000	18.3 (γ-FeOOH)	100 - 200 (needle)	spherical + neddle	anionic polymer	$FeSO_4^+$	2.56	//////////	0.033	//////////	3	
PSS 500,000	14.4	100 - 200 (needle)	spherical + neddle	anionic polymer	$FeSO_4^+$	2.56	//////////	0.017	//////////	2.2	
PAA 5000	11.4 (γ-FeOOH)	100 - 200 (needle)	spherical + neddle	anionic polymer	$Fe(CH_3COO)^{2+}$	3.38	//////////	0.042	//////////	0.2	
PAA 25,000	8.5	100 - 200 (needle)	spherical + neddle	anionic polymer	$Fe(CH_3COO)^{2+}$	3.38	//////////	0.065	//////////	0.49	
PEI 600	19.3		spherical + neddle	cationic polymer	//////////	//////////	//////////	0.038	55.9	2.3	
PEI 1800	Not measured (α-FeOOH)	the largest spherical size	spherical + neddle	cationic polymer	//////////	//////////	//////////	0.049	8.73	0.29	
PEI 10,000	Not measured (α-FeOOH)		neddle	cationic polymer	//////////	//////////	//////////	0.06	0.885	0.49	

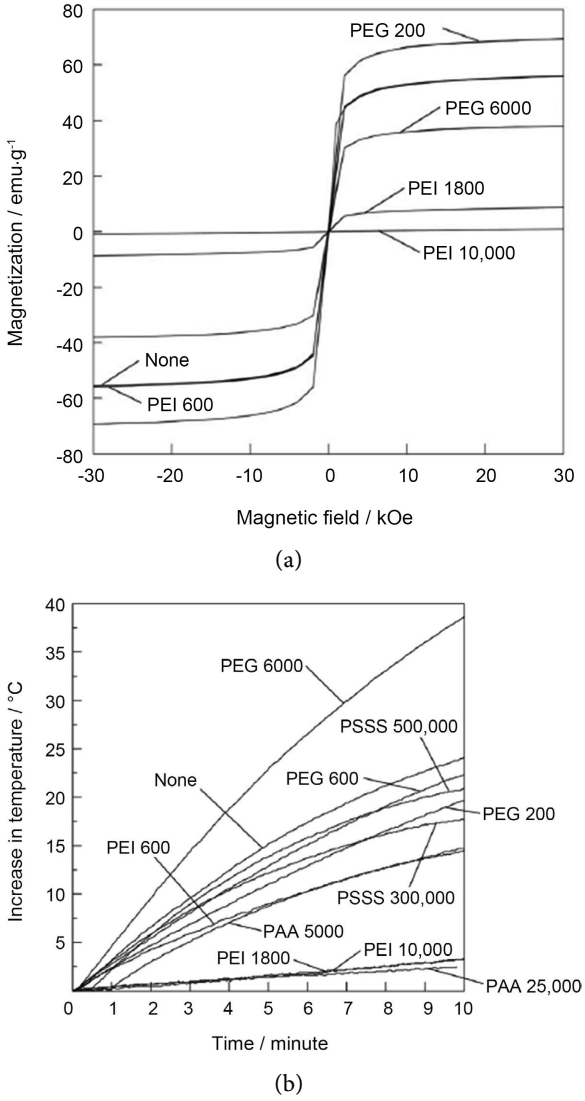

Figure 3. (a) Magnetization at room temperature, (b) Temperature rise under AMF [27].

Darwish *et al.* [28] reported in their elegant work the synthesis of polyvinyl alcohol coated magnetite for hyperthermia application with the objective to improve the heating efficiency under an alternating magnetic field. The size, magnetization and the SAR values for bare-MNPs and PVA-MNPs are summarized in **Table 3**. As can be seen from the data, the MNPS have small size with spherical shape. The authors observed that coating magnetite with PVA is benefit in terms of magnetization and also SAR values. Saturation increases from 41 emu/g for un-coated to 45 emu/g for PVA coated MNPs, this increase of saturation leads to the improvement of SAR value which increase considerably. Darwish and co-authors showed that heat dissipated by MNPs can be tuned by changing the field amplitude or frequency of the applied field as shown in **Figure 4(a)-(e)**. The observed an increase of SAR and temperature rise with increasing field amplitude and frequency (**Figure 4(f)**).

Table 3. The main parameters of coated and uncoated MNPs [28].

Sample	core size (nm)	Morphology	Zeta potential (mV)	Ms (emu/g)	SAR (W/g)
Bare-MNPs	12.3 ± 3.2	spherical shape		41.98	4.84
MNPs@PVA	10 ± 2.5	spherical shape	−11.49	45.08	163.81

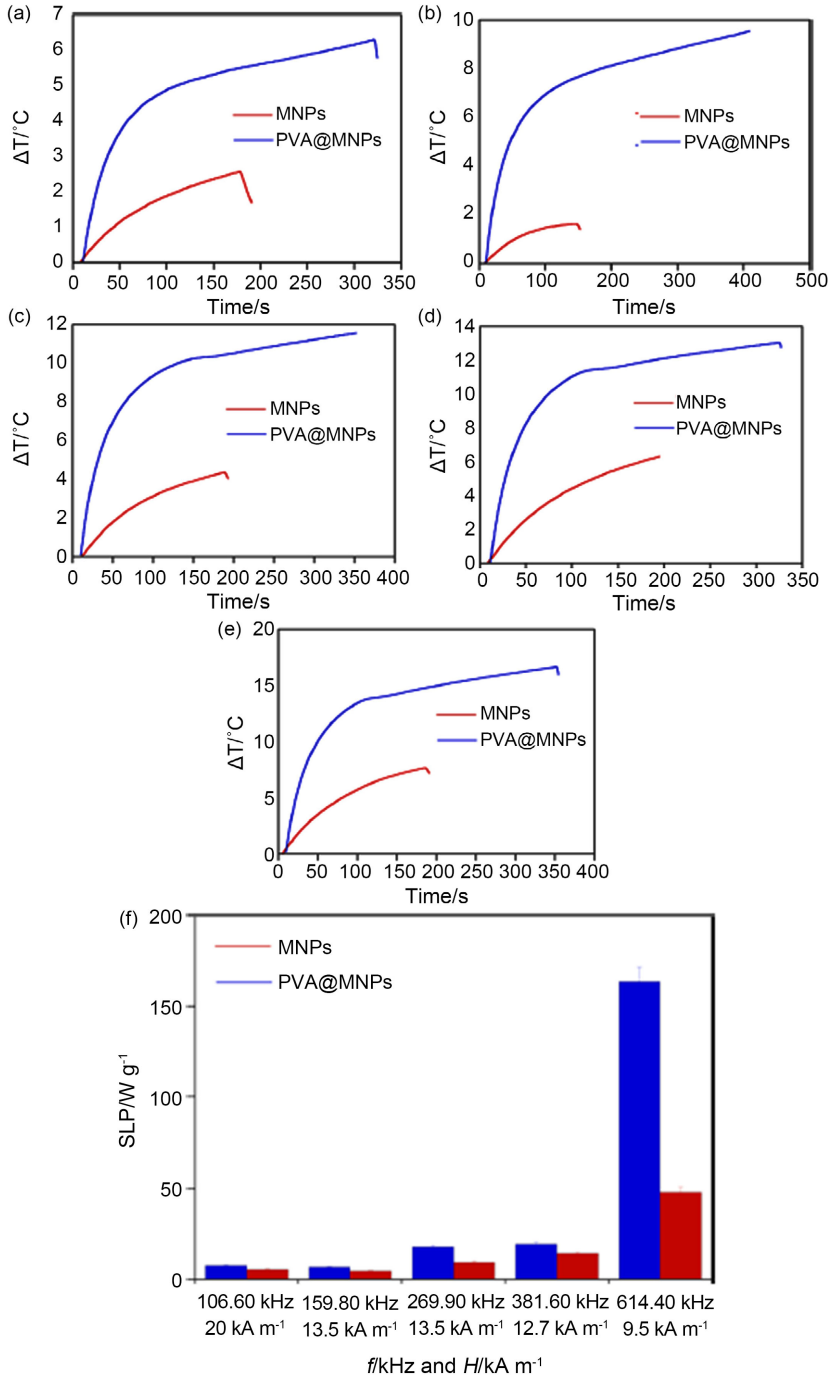

Figure 4. Heating efficiency for MNPs and PVA@MNPs at the conditions: (a) f = 106.6 kHz and H = 20 kA·m^{-1}, (b) f = 159.8 kHz and H = 13.5 kA·m^{-1}, (c) f = 269.9 kHz and H = 13.5 kA·m^{-1}, (d) f = 381.6 kHz and H = 12.7 kA·m^{-1} and (e) f = 614.4 kHz and H = 9.5 kA·m^{-1} and (f) SAR corresponding [28].

6. Conclusion

In summary, coating magnetite nanoparticles by polymers in an efficient approach to tune the structural, magnetic properties and subsequently their heating ability for magnetic hyperthermia. Types of polymers play a major role in the desired properties. We observed that coating magnetite with PVA improved the magnetization and leads to enhancement of SAR values. Similar effect was observed when magnetite nanoparticles are functionalized by PVP. It was found that both saturation and SAR increase drastically compared to the values of un-coated MNPs. It was found also that coating with some other polymers such as PAA or chitosan reduce the magnetization due the magnetic dead layers induced by the polymers.

Conflicts of Interest

The author declares no conflicts of interest regarding the publication of this paper.

References

[1] Strakhov, I.S., Mezhuev, Y.O., Korshak, Y.V., Kovarskii, A.L. and Shtil'man, M.I. (2016) Preparation of Magnetite Nanoparticles Modified with Poly(o-Phenylenediamine) and Their Use as Drug Carriers. *Russian Journal of Applied Chemistry*, **89**, 447-450. https://doi.org/10.1134/S1070427216030150

[2] Gupta, A.K. and Gupta, M. (2005) Synthesis and Surface Engineering of Iron Oxide Nanoparticles for Biomedical Applications. *Biomaterials*, **26**, 3995-4021. https://doi.org/10.1016/j.biomaterials.2004.10.012

[3] Wu, W., Wu, Z., Yu, T., Jiang, C. and Kim, W.S. (2015) Recent Progress on Magnetic Iron Oxide Nanoparticles: Synthesis, Surface Functional Strategies and Biomedical Applications. *Science and Technology of Advanced Materials*, **16**, Article ID: 023501. https://doi.org/10.1088/1468-6996/16/2/023501

[4] Kolhatkar, A.G., Jamison, A.C., Litvinov, D., Willson, R.C. and Lee, T.R. (2013) Tuning the Magnetic Properties of Nanoparticles. *International Journal of Molecular Sciences*, **14**, 15977-16009. https://doi.org/10.3390/ijms140815977

[5] Jordan, A., Scholz, R., Wust, P., Schirra, H., Schiestel, T., Schmidt, H., *et al.* (1999) Endocytosis of Dextran and Silan-Coated Magnetite Nanoparticles and the Effect of Intracellular Hyperthermia on Human Mammary Carcinoma Cells *in Vitro*. *Journal of Magnetism and Magnetic Materials*, **194**, 185-196. https://doi.org/10.1016/S0304-8853(98)00558-7

[6] Zhu, W., Wang, D., Xiong, J., Liu, J., You, W., Huang, J., *et al.* (2015) Study on Clinical Application of Nano-Hydroxyapatite Bone in Bone Defect Repair. *Artificial Cells, Nanomedicine, and Biotechnology*, **43**, 361-365. https://doi.org/10.3109/21691401.2014.893521

[7] Karimzadeh, I., Aghazadeh, M. and Shirvani-Arani, S. (2016) Preparation of Polymer Coated Superparamagnetic Iron Oxide. *International Journal of Bio-Inorganic Hybrid Nanomaterials*, **5**, 33-41.

[8] Pana, O., Teodorescu, C., Chauvet, O., Payen, C., Macovei, D., Turcu, R., *et al.* (2007) Structure, Morphology and Magnetic Properties of Fe-Au Core-Shell Nanoparticles. *Surface Science*, **601**, 4352-4357.

https://doi.org/10.1016/j.susc.2007.06.024

[9] Castello, J., Gallardo, M., Busquets, M.A. and Estelrich, J. (2015) Chitosan (or Alginate)-Coated Iron Oxide Nanoparticles: A Comparative Study. *Colloids and Surfaces A*: *Physicochemical and Engineering Aspects*, **468**, 151-158. https://doi.org/10.1016/j.colsurfa.2014.12.031

[10] Wu, W., He, Q. and Jiang, C. (2008) Magnetic Iron Oxide Nanoparticles: Synthesis and Surface Functionalization Strategies. *Nanoscale Research Letters*, **3**, Article No. 397. https://doi.org/10.1007/s11671-008-9174-9

[11] Kandpal, N., Sah, N., Loshali, R., Joshi, R. and Prasad, J. (2014) Co-Precipitation Method of Synthesis and Characterization of Iron Oxide Nanoparticles. https://www.semanticscholar.org/paper/Co-precipitation-method-of-synthesis-and-of-iron-Kandpal-Sah/3f921e7ec8e27a698675080ec115368f0319ec0f

[12] Jolivet, J.P., Chanéac, C. and Tronc, E. (2004) Iron Oxide Chemistry. From Molecular Clusters to Extended Solid Networks. *ChemInformChemInform*, **35**, 481-487. https://doi.org/10.1002/chin.200418249

[13] Hassan, P.A., Rana, S. and Verma, G. (2015) Making Sense of Brownian Motion: Colloid Characterization by Dynamic Light Scattering. *Langmuir*, **31**, 3-12. https://doi.org/10.1021/la501789z

[14] Lu, X.Y., Wu, D.C., Li, Z.J. and Chen, G.Q. (2011) Polymer Nanoparticles. *Progress in Molecular Biology and Translational Science*, **104**, 299-323. https://doi.org/10.1016/B978-0-12-416020-0.00007-3

[15] Lim, J., Yeap, S.P., Che, H.X. and Low, S.C. (2013) Characterization of Magnetic Nanoparticle by Dynamic Light Scattering. *Nanoscale Research Letters*, **8**, Article No. 381. https://doi.org/10.1186/1556-276X-8-381

[16] Clogston, J.D. and Patri, A.K. (2011) Zeta Potential Measurement. In: McNeil, S.E., Ed., *Characterization of Nanoparticles Intended for Drug Delivery*, Humana Press, Totowa, 63-70. https://doi.org/10.1007/978-1-60327-198-1_6

[17] Kroon, R.E. (2013) Nanoscience and the Scherrer Equation versus the "Scherrer-Gottingen Equation". *South African Journal of Science*, **109**, Article #a0019. https://pdfs.semanticscholar.org/0000/94a98be6e96aedcec3a3a93077d5da3e5778.pdf

[18] Langford, J.I. and Wilson, A.J.C. (1978) Scherrer after Sixty Years: A Survey and Some New Results in the Determination of Crystallite Size. *Journal of Applied Crystallography*, **11**, 102-113. https://doi.org/10.1107/S0021889878012844

[19] Uvarov, V. and Popov, I. (2013) Metrological Characterization of X-Ray Diffraction Methods at Different Acquisition Geometries for Determination of Crystallite Size in Nano-Scale Materials. *Materials Characterization*, **85**, 111-123. https://doi.org/10.1016/j.matchar.2013.09.002

[20] Mansfield, E., Tyner, K.M., Poling, C.M. and Blacklock, J.L. (2014) Determination of Nanoparticle Surface Coatings and Nanoparticle Purity Using Microscale Thermogravimetric Analysis. *Analytical Chemistry*, **86**, 1478-1484. https://doi.org/10.1021/ac402888v

[21] Babincova, M., Leszczynska, D., Sourivong, P., Cicmanec, P. and Babinec, P. (2001) Superparamagnetic Gel as a Novel Material for Electromagnetically Induced Hyperthermia. *Journal of Magnetism and Magnetic Materials*, **225**, 109-112. https://doi.org/10.1016/S0304-8853(00)01237-3

[22] Kallumadil, M., Tada, M., Nakagawa, T., Abe, M., Southern, P. and Pankhurst, Q.A., (2009) Suitability of Commercial Colloids for Magnetic Hyperthermia. *Journal of Magnetism and Magnetic Materials*, **321**, 1509-1513. https://doi.org/10.1016/j.jmmm.2009.02.075

[23] El-Boubbou, K., Lemine, O.M., Ali, R., Huwaizi, S.M., Al-Humaid, S. and AlKushi, A. (2022) Evaluating Magnetic and Thermal Effects of Various Polymerylated Magnetic Iron Oxide Nanoparticles for Combined Chemo-Hyperthermia. *New Journal of Chemistry*, **46**, 5489-5504. https://doi.org/10.1039/D1NJ05791J

[24] Algessair, S., Lemine, O.M., Madkhali, N., *et al.* (2023) Tuning the Heat Dissipated by Polyacrylic Acid (PAA)-Coated Magnetite Nanoparticles under Alternating Magnetic Field for Hyperthermia Applications. *Applied Physics A*, **129**, Article No. 814. https://doi.org/10.1007/s00339-023-07097-9

[25] Fatima, H., Charinpanitkul, T. and Kim, K.S. (2021) Fundamentals to Apply Magnetic Nanoparticles for Hyperthermia Therapy. *Nanomaterials*, **11**, Article 1203. https://doi.org/10.3390/nano11051203

[26] Sadat, M.E., Patel, R., Sookoor, J., Bud'ko, S.L., Ewing, R.C., Zhang, J., Xu, H., Wang, Y., Pauletti, G.M., Mast, D.B. and Shi, D. (2014) Effect of Spatial Confinement on Magnetic Hyperthermia via Dipolar Interactions in Fe_3O_4 Nanoparticles for Biomedical Applications. *Materials Science and Engineering: C*, **42**, 52-63. https://doi.org/10.1016/j.msec.2014.04.064

[27] Miyazaki, T., Tange, T., Kawashita, M. and Jeyadevan, B. (2020) Structural Control of Magnetite Nanoparticles for Hyperthermia by Modification with Organic Polymers: Effect of Molecular Weight. *RSC Advances*, **10**, 26374-26380. https://doi.org/10.1039/D0RA04220J

[28] Thorat, N.D., Lemine, O.M., Bohara, R.A., Omri, K., El Mir, L. and Tofail, S.A. (2016) Superparamagnetic Iron Oxide Nanocargoes for Combined Cancer Thermotherapy and MRI Applications. *Physical Chemistry Chemical Physics*, **18**, 21331-21339. https://doi.org/10.1039/C6CP03430F